MASTER

STATUS REPORT TO DOE NUCLEAR DATA COMMITTEE

Robert C. Haight
Cordon L. Struble

March 13, 1980

Lawrence
Livermore
Laboratory

LAWRENCE LIVERMORE LABORATORY

A. <u>NUCLEAR DATA APPLICATIONS - MEASUREMENTS</u>

1. <u>Neutron Total Cross Section for Tritium</u>. (Phillips, Berman, and Seagrave*)

We have measured the neutron total cross section for tritium, for incident neutron energies ranging from 60 keV to 80 MeV at the LLL linac, using a high-pressure gas sample and the neutron time-of-flight technique, with an experimental accuracy of better than 0.5% over much of this energy range. Similar measurements on hydrogen and deuterium also were performed.[1,2]

The cross-section data obtained for tritium (Fig. A-1) lead to the following conclusions: (1) the extrapolated zero-energy cross section is found to be 1.70 ± 0.03 b, in sharp disagreement with previous thermal-energy observations, but in agreement with calculations which also yield the currently-accepted coherent scattering length, 3.73 fm, (2) a minimum in the cross section near 600 keV (with a rise at lower energy) is newly observed, (3) agreement with a prediction from an analysis of p-^{3}He data is within 1% at the resonance peak near 3.5 MeV, but the data differ from this prediction by as much as 6% at lower and higher energies, and (4) the cross section in the heretofore unexplored energy region between 7 and 14 MeV exhibits no structure, thus contradicting the existence of a bound four-neutron state.

2. <u>Photodisintegration of Tritium</u> (Berman, Faul, Meyer, and Olson)

We have measured both the two-body (γ,n) and three-body (γ,2n) photodisintegration cross sections for tritium, for incident photon energies from threshold to ∿25 MeV at the LLL linac, using a high-pressure gas sample and monoenergetic photons from the annihilation in flight of fast positrons with photon resolution between 1 and 2%, with an experimental accuracy between 7 and 10%.[3,4] This is the first measurement of

---

*Los Alamos Scientific Laboratory, Los Alamos, NM 87545.

[1] J. D. Seagrave, B. L. Berman, and T. W. Phillips, Physics Letters B (to be published) and UCRL-83891 (1980).

[2] T. W. Phillips, B. L. Berman, and J. D. Seagrave, UCRL-77783 (1979).

[3] D. D. Faul, B. L. Berman, P. Meyer, and D. L. Olsen, Phys. Rev. Letters 44, 129 (1980).

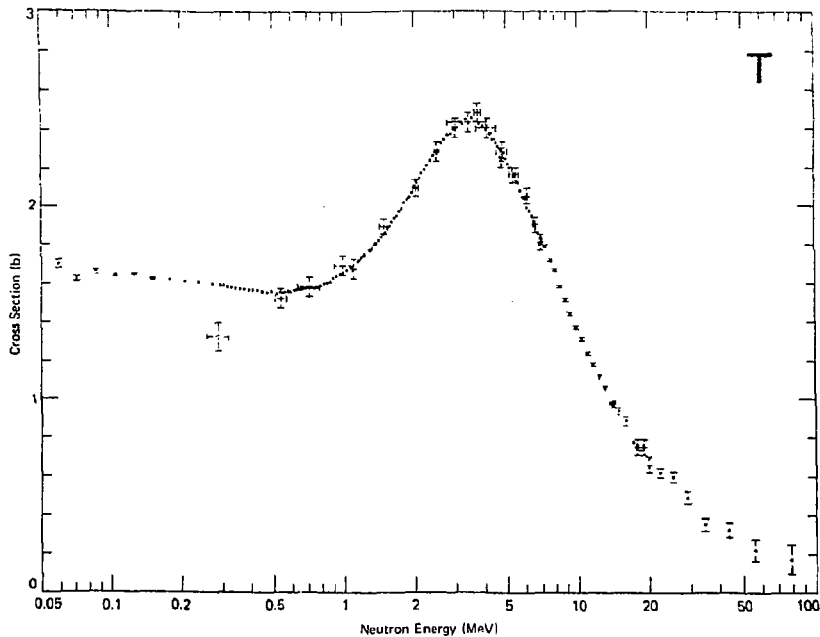[4] B. L. Berman, D. D. Faul, P. Meyer, and D. L. Olsen, UCRL-82188 (1979).

Figure A-1. Total cross section for tritium. The data indicated with crosses are literature values; those with points are present results.

these cross sections across the energy region of their maxima. Similar
measurements on deuterium, oxygen, and the helium isotopes also were per-
formed. Presently available calculations for the tritium cross sections
are not adequate to explain the measured cross sections.

3. **Photoneutron Cross Sections for ^{17}O** (Berman, Faul, Meyer,
Woodworth, and Jury*)

We have measured the photoneutron [(γ,n) and $(\gamma,2n)$] cross
sections for ^{17}O from 8 to 40 MeV at the LLL linac, using a water sam-
ple and monoenergetic photons from the annihilation in flight of fast
positrons with photon resolution between 1 and 2%, with an experimental
accuracy of 7%. Similar measurements on ^{13}C and ^{18}O have been reported
and published previously; measurements on ^{16}O were performed simultane-
ously with those on ^{17}O;[5] and others, on ^{15}N, ^{29}Si, and ^{30}Si, will be
performed later this year.

4. **Measurements of ^{88}Sr(p,n) to the Ground State and Low-Lying
Excited States of ^{88}Y** (Grimes, Poppe, and Wong)

In order to extract the (n,p) cross section for the unstable
nuclide ^{88}Y (107 day) we have measured the inverse (p,n) cross section
on the stable target ^{88}Sr for proton energies between 5.75 and 11 MeV.
Protons from the LLL model-EN tandem Van de Graaff accelerator bom-
barded a metallic foil target and neutrons were detected using a 16-
detector time-of-flight spectrometer. The detectors, NE213 liquid scin-
tillators, spanned angles between 3.5° and 160° and were located at a
flight path of 10.5 m. Overall resolution was sufficient to separate
the ^{88}Y ground state ($J^\pi = 4^-$), the first excited state ($J^\pi = 5^-$) at
0.232 MeV, and the second excited state ($J^\pi = 1^+$) at 0.393 MeV. Higher
unresolved states were also observed. A Legendre polynomial fit was
made to the angular distributions and the resulting integrated cross
sections are shown in Fig. A-2. From the principle of detailed balance,
the inverse cross sections ^{88}Y(n,p) ^{88}Sr(g.s.) may be extracted from
these data for the ^{88}Y ground state and the 0.3-ms isomer at 0.393 MeV.
The data may also be used as a basis for Hauser-Feshbach calculations
which will allow the total (n,p) cross section on the ^{88}Y ground state
and important isomers to be estimated.

*Trent University, Peterborough, Ontario, Canada.

[5] J. W. Jury, B. L. Berman, D. D. Faul, P. Meyer, J. G. Woodworth,
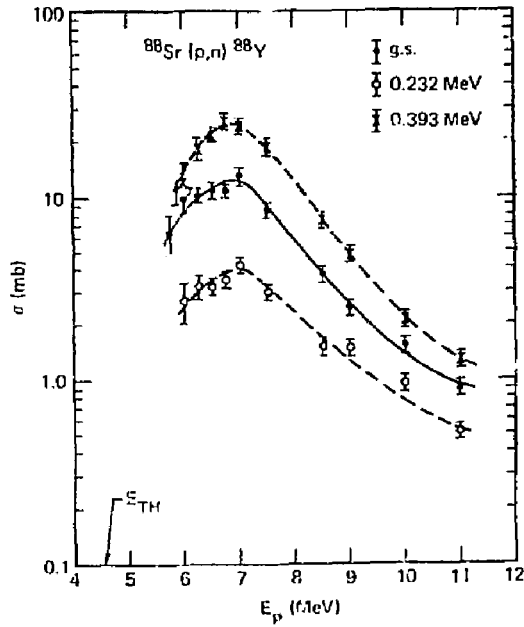Phys. Rev. C21, 503 (1980).

Figure A-2. Angle-integrated cross sections as a function
of bombarding energy for the ^{88}Sr(p,n) reaction to the
ground state (g.s.) of ^{88}Y and the first two excited states
(E_x = 0.232 and 0.393 MeV). The curves serve only to
connect the data and guide the eye. The arrow near 4.4 MeV
indicates the threshold for the g.s. reaction.

5. Information on Gamma-Ray Strength Functions in the Mass-90
    Region from Proton-Induced Reactions (Dietrich, Heikkinen, and
    Gardner)

        In order to understand the systematics of gamma-ray production
we have extended our measurements in the mass-90 region to include exci-
tation functions and spectral distributions of gammas produced by proton
bombardment of ^{92,96,100}Mo. Data were taken from 3 MeV to energies well
above the (p,n) thresholds. Gamma rays were detected with Ge(Li) and
anticoincidence-shielded NaI spectrometers. The Ge(Li) detector was
used to obtain individual gamma lines from transitions between low-lying
states in the compound nucleus and from transitions following the (p,n)
and (p,p') reactions where energetically possible. The NaI spectrometer
was used to obtain the entire gamma-ray spectrum and the total energy
released as gammas. Previous measurements on ^{88}Sr, ^{89}Y, and ^{90}Zr have
shown that the excitation functions of individual gamma lines and the
total energy released by gammas is reproduced reasonably well by standard
Hauser-Feshbach calculations. However, the gamma spectral distributions
require a modification of the energy-dependence of the E1 gamma-strength
function from the usual Brink-Axel (Lorentzian) form. Such a modifica-
tion is described elsewhere in this report and is being applied to calcu-
lations in the mass-90 region.

6. Studies of (n, charged particle) Reactions with 14-15 MeV
    Neutrons (Haight, Grimes, and Barschall*)

        Materials bombarded by fusion neutrons are altered by nuclear
transmutations that produce hydrogen and helium. To assess the potential
performance of these materials for fusion reactor application, cross
section data are required by the fusion community and the Office of
Fusion Energy. Under the sponsorship of the DOE Office of Basic Energy
Sciences, we measure these quantities by detecting the charged particles
emitted by materials under bombardment by neutrons of 14 to 15 MeV.
By also measuring the energy and angular distributions of the charged
particles, we are able to test nuclear reaction theories through model
calculations and to deduce KERMA factors for consideration of energy
deposition by the neutrons.

        In the past year we have measured Y, Zr, ^{92,94,95,96}Mo, C, ^{7}Li,
and F. Together with our previous data the heavier targets complete most
top priority materials for structural application for neutron energies
in the 14-15 MeV region. A proton spectrum from ^{94}Mo is shown in
Fig. A-3. The lighter targets have been measured at 14 MeV with a coni-
cal neutron-producing rotating target. To calibrate the response of the
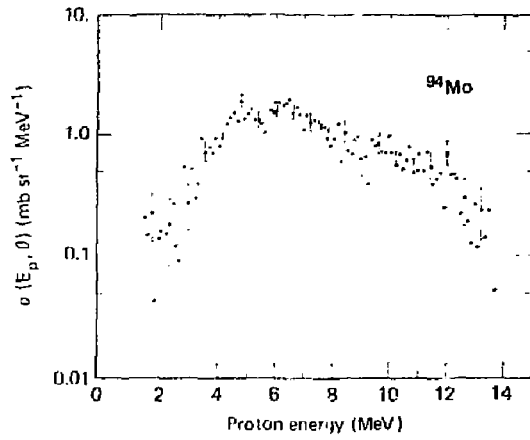
_____

*University of Wisconsin, Madison, WI 53706.

Figure A-3. Spectrum of protons emitted at 90°
from ^{94}Mo under bombardment with 15-MeV neutrons.

spectrometer for low-energy alpha particles emitted by the light targets, we have developed a high-pressure thin-window helium gas cell.[6] The n-alpha elastic scattering cross section is taken to be the standard for this calibration.

7. Neutron Total Cross Section Measurements from 2.5 to 60 MeV (Camarda,* Phillips, and White)

Using the Lawrence Livermore Laboratory 100-MeV electron linear accelerator in conjunction with a 250-meter flight path we have measured at the 1-3% level the absolute neutron total cross section of ^{140}Ce and at the 0.3% level the relative cross sections $^{142}Ce/^{140}Ce$ and $^{141}Pr/^{140}Ce$. The samples were in oxide form. For the ^{140}Ce absolute cross section measurement, an H_2O sample with an equivalent amount oxygen formed the open. The effect of the hydrogen was unfolded analytically. For these measurements the neutron-producing target was made of TaBe and the detector consisted of 16 independent plastic scintillators (25cmx25cmx5cm). Optical model calculations are being performed and will be compared with the data.

8. Measurement of the (p,n) Reaction to the Ground- and Excited-Analog States of Se Isotopes (Wong, Pohl, Poppe, and Rhodes)

In recent years we have attempted to deduce neutron scattering by applying the Lane model to measured (p,n) cross sections for charge-exchange to the isobaric analog state of the target nucleus.[7] It was discovered that multi-step processes proceeding through excited states of the target and excited analog states have a pronounced effect on the ground-state transition[8] and must be understood if the Lane model is to be successfully applied. By using a coupled-channel calculation, we are able to reproduce the charge-exchange cross sections to excited analog states using only parameters derived from proton inelastic scattering and results of the ground-state analog measurements.[9] Because of the good agreement between the experiments and calculations, we believe that measurements of (p,n) charge-exchange cross sections will allow us to

*Penn State University, Delaware Campus, Media, PA 19063.

[6] R. C. Haight, C. Rambo, J. Cormier, and J. L. Garibaldi, Nucl. Instr. and Meth. 164, 613 (1979).

[7] C. Wong et al., Phys. Rev. C5, 158 (1972); C. Wong et al., Phys. Rev. C7, 1895 (1973); S. M. Grimes et al., Phys. Rev. C11, 158 (1975).

[8] V. A. Madson et al., Phys. Rev. C13, 548 (1976).

[9] C. Wong et al., Phys. Rev. C20, 59 (1979).

deduce both neutron elastic and inelastic scattering. We are continuing
to study this hypothesis and recently have completed measurements on the
isotopes ^{76,80,82}Se for proton energies of 19, 22, and 25 MeV. In this
experiment the isobaric analogs of the ground states of the target nuclei
were observed as well as the one- and two-phonon excited analogs for the
Se isotopes.

9. Level Structure and Octupole Bands in ^{180}W (Mann, Carlson,
Lanier, Struble, Buckley, Heikkinen, Proctor, and Singh)

In a study of ^{180}W using the ^{181}Ta($p,2n\gamma$)^{180}W reaction, we pro-
duced states up to I = 12 and were able to establish the details of the
K^{π} = 2^{-} octupole band up to the 11^{-} state.[10] Several other rotational
bands were observed, including the previously-studied band built on the
metastable K^{π} = 8^{-} state at 1529 keV, the γ-vibrational bands, and a new
band built on a K = 5 state at 1639.8 keV. We also observed a state at
1634.5 keV which we tentatively interpreted as the K^{π} = 3^{-} octupole band
head, based on its decay properties and on the likely possibility that it
is the same state as one observed near 1637 keV in the (d,d') reaction.

A confusing result from this study was our inability to identify
the K = 0 and K = 1 components of the octupole vibration. In an attempt
to understand this we performed a Hauser-Feshbach calculation using
standard proton and neutron optical parameters and γ-ray strength func-
tions.[11] The calculation, which utilized all the known or predicted
levels up to 2.5 MeV, gave generally good agreement with our observed
γ-ray intensities and indicated that population of the K = 1 octupole
band should be easily observable, while population of the K = 0 band
would be too weak. We therefore made a further search for the bands
using the decay of ^{180}Re.

Rhenium-180 decays to ^{180}W by β emission from the J^{π} = 1^{-} ground
state with a Q-value of ~3800 keV. Therefore, we might expect the decay
to populate states in ^{180}W having J^{π} = 0^{-} and 1^{-} (as well as 2^{-}). In the
decay study, we were able to identify states up to 2.9 MeV. None of the
states above 1232.7 keV had been observed previously except the one at
1831.7 keV. The states at 1587.25 and 1632.90 keV, and a state at 1693.6
keV observed both in the (p,2nγ) study and in (d,d') excitation, could
be the first three members of the K^{π} = 1^{-} octupole band. More specula-
tively, the state at 1814.9 keV, which agrees very closely in energy with
a state seen in (d,d') excitation, could possibly be the I = 3 member of
the J^{π} = 0^{-} octupole bands. These conclusions would be consistent with

10 L. G. Mann, J. B. Carlson, R. G. Lanier, G. L. Struble, W. M. Buckley,
   D. W. Heikkinen, I. D. Proctor, and R. K. Sheline, Phys. Re.. C19,
   1191 (1979).

11 D. G. Gardner, Report No. UCRL-76253, 1975 (unpublished).

the results of the Hauser-Feshbach calculation, i.e., the population of the 1693.6-keV state in the (p,2nγ) experiments agrees well with the predictions for I = 3 member of the $K^{\pi} = 1^-$ band.

10. Neutron-Capture Cross Sections for Osmium Isotopes (Berman and Browne*)

We have measured the neutron-capture cross sections for ^{186}Os, ^{187}Os, ^{188}Os, ^{189}Os, ^{190}Os, and ^{192}Os for neutron energies from 0.5 eV to 150 keV at the LLL linac, using powdered-metal samples and the neutron-time-of-flight technique, with an experimental accuracy of 5%.[12] The ratio of the Maxwellian-weighted average cross sections for ^{186}Os and ^{187}Os near 30 keV is a vital parameter for the determination of the duration of nucleosynthesis prior to the formation of the solar system, and thus, for the determination by the nuclear-dating technique of the age of the universe. The present result of 17 ± 4 x 10^9 y is in concordance with the values obtained from U-Th dating and from the globular-cluster method, but clearly exceeds the most recent determination of the Hubble time.

11. Pulsed Sphere Tests of the ENDF/B-V Cross Sections for Cu, Nb, ^{232}Th and ^{238}U (Hansen, Wong, Komoto, Pohl, and Howerton)

The time-of-flight measurements of the neutron emission spectra from pulsed spheres of Cu (1.0, 3.0 and 5.0 mfp), Nb (1.0 and 3.0 mfp), ^{232}Th (1.0 mfp), and ^{238}U (1.0 and 3.0 mfp), bombarded with 14-MeV neutrons, were reported in the 1979 Status Report, together with Monte Carlo calculations using the ENDF/B-IV library. These calculations were carried out with TARTNP, a coupled neutron-photon transport code.

For the recent version V of the ENDF/B library, the cross sections for Cu, ^{232}Th and ^{238}U have been reevaluated. (The Nb evaluation is the same in versions IV and V.) We present here a comparison between the above measurements and the TARTNP calculations using the new cross sections.

The measured integrals and the ratios of calculated to measured integrals for the energy intervals 0.8 to 5, 5 to 10, and 10 to 15 MeV are tabulated in Table A-1. The ratios calculated with the ENDF/B-IV library are also given for purposes of comparison between versions IV and V. The comparisons between the measurements and the calculations show that, with the exception of ^{232}Th where an appreciable improvement

---

*Present address: Los Alamos Scientific Laboratory, Los Alamos, NM 87545.

[12] A brief description is in: J. C. Browne and B. L. Berman, Nature 262, No. 5565, 197 (1976).

Table A-1. Measured integrals and ratios (RIV, RV) of calculated (ENDF/B-IV, ENDF/B-V) to measured integrals.

Material	E MeV	Exp ±7%	RIV	RV	Exp ±7%	RIV	RV	Exp ±7%	RIV	RV
			1 mfp			3 mfp			5 mfp	
Cu	0.8-5	0.313	0.898	0.895	0.465	0.815	0.802	0.285	0.737	0.723
	5.0-10	0.041	0.610	0.537	0.037	0.514	0.459	0.017	0.588	0.412
	10.0-15	0.642	0.988	0.964	0.236	0.949	0.886	0.082	0.915	0.780
Nb	0.8-5	0.308	0.763	a	0.422	0.628	a			
	5.0-10	0.031	0.581	a	0.033	0.636	a			
	10.0-15	0.707	0.987	a	0.265	0.898	a			
^{232}Th	0.8-5	0.442	1.057	1.048						
	5.0-10	0.039	0.513	1.000						
	10.0-15	0.645	0.974	1.008						
^{238}U	0.8-5	0.670	0.888	0.984	0.803	1.054	1.159			
	5.0-10	0.059	0.780	0.610	0.063	0.825	0.635			
	10.0-15	0.669	0.964	0.967	0.232	1.022	1.052			

a) The ENDF/B-IV and V libraries are identical for Nb.

Figure A-4. Neutron emission spectrum measured by time of flight from a 1 mfp ^{232}Th sphere compared with calculations based on the ENDF/B-IV and ENDF/B-V libraries.
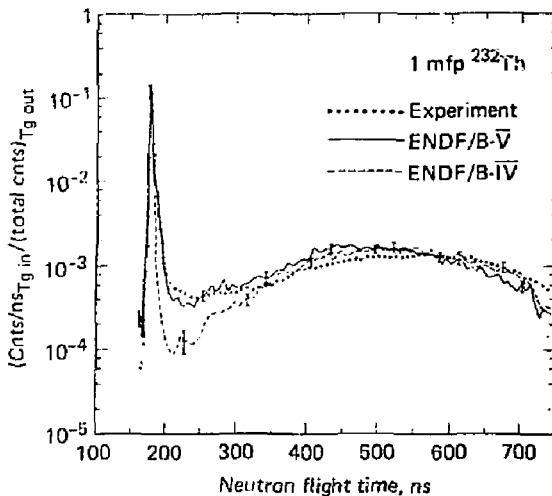
in the fit to the measurements has been achieved with the new cross sections (see Fig. A-4), the changes in the cross sections between the B-IV and B-V library do not reduce the discrepancies between measurements and calculations pointed out earlier for version IV of the library. In particular the B-V calculations continue to underestimate the neutron production between 5 and 10 MeV for Cu and ^{238}U. The discrepancies vary from up to 59% for Cu to 37% for ^{238}U.

A detailed discussion of the cross section changes between the two libraries and the reasons for the persistence of the discrepancies is given in Ref. 13.

12. Proton Inelastic Scattering in the Actinide Region (Hansen, Proctor, Madsen, Pohl, and Brown)

Elastic and inelastic proton differential cross sections have been measured for ^{232}Th and ^{238}U at 20 and 26 MeV, using the proton beam from the 'LL cyclograaff facility. From these data and nuclear model calculations we hope to understand more fully the corresponding neutron scattering cross sections as well as (p,n) reactions. Proton groups corresponding to levels up to 6$^+$ in the ground state rotational band of ^{232}Th and up to 8$^+$ in ^{238}U have been measured with an Enge split-pole spectrograph. The data have been analyzed using coupled-channel calculations for deformed nuclei with the Oregon-State code, updated by Madsen and Brown.

We have studied the sensitivity of the results: (a) to the optical parameters used in the calculations, (b) to the shape of the nuclear charge distribution (a deformed homogeneous or a deformed Fermi distribution), (c) to the type of coupling assumed among the levels (i.e. quadrupole and/or hexadecapole for the 4$^+$, 6$^+$ levels), (d) to the type of expansion (a Taylor power series or a Legendre polynomial) used for the nuclear and Coulomb potentials, and (e) to the magnitude of the deformation parameters, β_N and β_C used for the nuclear and Coulomb potentials.

From the fits to the data we have determined the best choice among conditions b-d, and the best set of optical and deformation parameters. These results will be used in the analysis of the (p,n) cross sections at 26 MeV for ^{232}Th and ^{238}U isobaric analog states. These (p,n) measurements are in progress and the simultaneous analysis of the proton scattering and charge exchange data will allow us to infer neutron in-elastic cross sections for these nuclei.

---

[13] L. F. Hansen et al., Measurements and Calculations of the Neutron Emission Spectra from Materials used in Fusion-Fission Reactors (submitted for publication in Fusion Technology).

13. *Fission Cross Section of* ^{245}Cm (White, Browne*, Howe, and Landrum)

   As part of an ongoing series of measurements in the transplutonium mass region, the neutron-induced fission cross section of ^{245}Cm has been measured from 0.001 eV to 20 MeV using the LLL 100-MeV linac. The sample consisted of 190 µg of enriched (>99%) ^{245}Cm. A sample of ^{235}U was included in the measurement and was used to normalize the ^{245}Cm cross section above 10 keV. Below 10 keV the neutron flux was measured with a lithium glass detector and both the ^{245}Cm and ^{235}U data were reduced to relative cross sections by normalization to the measured flux shape. With the known 2200 m/sec ^{235}U fission cross section, the ratio of ^{245}Cm/^{235}U masses, and relative efficiencies of the fission chambers, the ^{245}Cm data were reduced to absolute cross sections.

   Errors (statistical) on the data are approximately 2% near thermal, 1% at 2 MeV and 5% at 14 MeV. The measured thermal fission cross section for ^{245}Cm in this experiment is 2080 barns.

   The data were analyzed in the resonance region with a multichannel R-matrix code with least-squares fitting capability. Preliminary resonance parameters have been obtained for levels below 32 eV. Figure A-3 shows fits to the ^{245}Cm fission data from 10 eV to 32 eV. The average fission width is 550 meV and the neutron strength function (1.02 x 10^{-4}) is in reasonable agreement with neighboring nuclei.

14. Fission Neutron Multiplicities for ^{245}Cm, ^{232}Th, and ^{242m}Am(n,f) Reactions (Howe, Browne*, White, Dupzyk, Landrum, and Dougan)

   Fission neutron multiplicities have recently been measured for neutrons incident on ^{245}Cm. Neutrons with energies between 10 keV and 20 MeV were produced with the electron linac. Typical uncertainties were 5% at 1 MeV and 25% at 15 MeV. A separate experiment was performed with this same accelerator to measure the neutron multiplicity near thermal energy to an accuracy of 1.7%. Preliminary results from both of these measurements fall below previous thermal values and typical rates of increase with incident neutron energy. To provide further confirmation of these numbers, a future experiment is being planned using a monoenergetic 14-MeV neutron source.

   Analysis is complete on the data from ^{232}Th(n,f) neutron multiplicity experiment. Results supplement existing measurements by filling in the unmeasured regions: 4.5-13 MeV, 17-40 MeV, and 1.0-1.2 MeV.

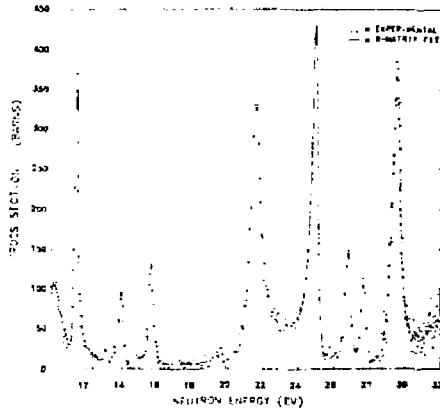*Present address: Los Alamos Scientific Laboratory, Los Alamos, NM 87545.

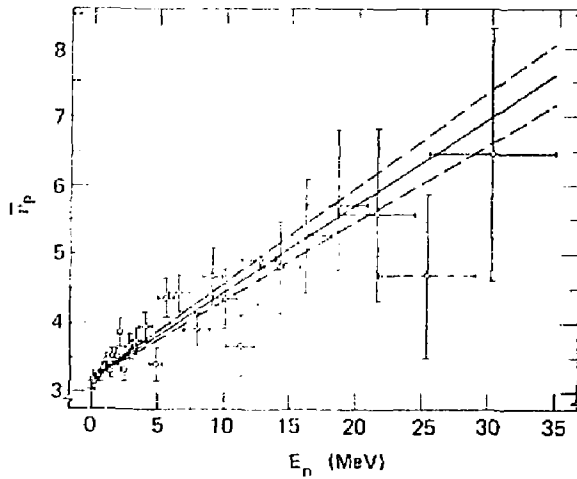Figure A-5. Fission cross section of ^{245}Cm from 10 to 32 eV.

Figure A-6. Fission neutron multiplicity of ^{242m}Am. The solid line represents a bivariant-weighted least-squares fit; the dashed lines indicate a confidence level of one standard deviation.

Previously-observed deviations from linearity below 2 MeV have been con-
firmed. While no unusual effects were observed near the (n,n'f) thres-
hold, a slight depression in the data does appear between 3 and 4 MeV.

Results from the ^{242m}Am(n,f) measurement are shown in Figure A-6.

B. NUCLEAR DATA APPLICATIONS - CALCULATIONS

1. A Study of the El Gamma-Ray Strength Function. (Gardner,
Gardner, and Dietrich)

Previously, we described systematics for the parameterization
of $f_{E1}(E_\gamma)$, the El gamma-ray strength function, in terms of the tail of
the giant dipole resonance (GDR), which was assumed to be Lorentzian in
shape.[14] The parameterization was tested in the mass-90 region by a
study of neutron and proton capture cross sections and the resulting
capture gamma-ray spectra.[15] We found that the capture cross sections
could be predicted fairly well, with perhaps two exceptions, but the
calculated gamma-ray spectra were invariably too "soft," i.e., lacking
in sufficient strength for the higher energy gamma rays.

It was felt that the problems concerning the spectral shapes
might be attributed to the choice of the Lorentz form for the extrapo-
lated tail of the GDR. This past year we have developed an alternate
form for the parameterization of the GDR,[16] and are in the process of
evaluating it, both in the mass-90 region[17] and also for nuclei from
Ta to Au.[16]

The GDR parameterization consists of two parts, the correlation
of the GDR parameters of peak energy, width and peak cross section for
elements from V to Bi, assuming two overlapping peaks with a separation
dependent upon deformation; and the description of the shape of each

[14] D. G. Gardner and M. A. Gardner, Neutron Capture Gamma-Ray Spectro-
scopy, ed. by R. E. Chrien and W. R. Kane, Plenum Press, New York,
1979, pp. 612-614.

[15] M. A. Gardner and D. G. Gardner, Proceedings of an International Con-
ference on Neutron Physics and Nuclear Data for Reactors and Other
Applied Purposes, Harwell, Sept., 1978, pp. 1121-1125. D. G. Gardner,
F. S. Dietrich, and D. W. Heikkinen, ibid., pp. 1126-1130.

[16] D. G. Gardner and F. S. Dietrich, UCRL-82998, Oct., 1979.

[17] M. A. Gardner and D. G. Gardner, UCRL-82999, Nov., 1979.

peak of the GDR with a Breit-Wigner form, but with an energy-dependent width.

$$\Gamma(E_\gamma) \;=\; \Gamma_R \; \left(\frac{C + E_X}{C + E_R} \right) \left(\frac{E_\gamma^{2}}{E_X} \right) \left(\frac{2}{E_X + E_R} \right) \tag{1}$$

Here Γ_R and E_R are the usual GDR width and peak energy, while C and E_X are global constants to be obtained by fitting spectral data. Thus the true damping width, $\Gamma(E_\gamma)$, was allowed to increase with gamma-ray energy until $\Gamma(E_\gamma) = \Gamma_R$, at which point the width was held constant for all higher energies.

An example of the new functional form is illustrated in Fig. B-1 in the case of ^{93}Nb(n,γ). The two energy-dependent Breit-Wigner (EDBW) curves represent different choices for the constant C in Eq. 1. Both EDBW curves produce "harder" gamma-ray spectra than the Lorentz curve. The results of our preliminary study show that the same values for the two constants, C and E_X, produce acceptable fits for both neutron capture cross sections and capture gamma-ray spectra, both in the mass-90 region and also in the Ta-Au mass region, and, in addition, produce agreement with the photonuclear data at higher gamma-ray energies.

2. Nuclear Level Densities (Grimes, Bloom, and Dalton[*])

The Fermi-gas model is the most extensively used approach to nuclear level densities. A more fundamental approach, however, would be to calculate the level densities from the two-body force. Not only would the connection between the force and level densities be explicit, but for practical calculations one could avoid empirical adjustments that the Fermi-gas model requires to account for shell effects.

We are investigating the calculation of nuclear level densities from the two-body force through the theory of spectral distributions. The level distribution in a finite basis is assumed to be Gaussian and can be characterized in terms of the total number of states, the average energy of the states ($<H>$) and the average energy squared of the states ($<H^2>$). Comparison of such an expansion with the eigenvalues obtained

---

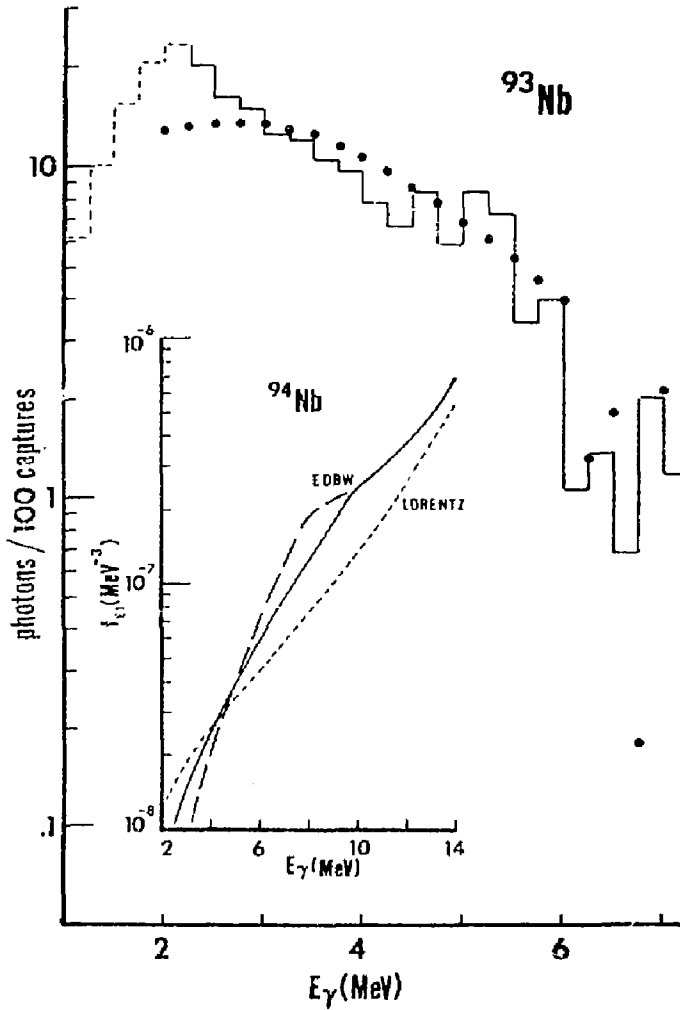[*]Ames Laboratory, USDOE, Ames, Iowa 50011.

Figure B-1. Comparison of measured thermal neutron capture gamma-ray spectrum for ^{93}Nb (histogram) with that calculated with the double-peak, EDBW model (solid circles). (Data source: V. J. Orphan et al., AD-717 (1970).) Insert compares f_{E1}'s for ^{94}Nb: Lorentz form (short-dashed curve), EDBW model (solid curve), and EDBW model with an extreme parameter set (long-dashed curve).

from diagonalization showed good agreement.[18] In more recent work[19] we found that the spectral distribution calculations compared fairly well with experimental data, but that terms additional to the Gaussian were needed to obtain the spin cutoff parameters. Work is presently under way to expand the capability of the level density codes to allow the calculation of third and higher moments of the Hamiltonian.

C. NUCLEAR DATA FOR REACTOR SAFETY

1. Determination of Properties of Short-Lived Fission Products (Meyer, Henry, and Lien)

Decay data on short-lived fission products are required to re-solve a number of problems associated with the design and operation of both thermal and fast reactors. Existing reactors cannot exceed power levels which are determined by the amount of heat generated in the core following a loss-of-coolant accident. This decay heat is produced by fission products and can be measured on a case-by-case basis or calcu-lated using summation calculations. These calculations depend on exist-ing data bases. In a program supported by DOE/BES we are measuring the decay properties of critical short-lived fission products in order to upgrade the ENDF/B data base. Existing plants must also carefully moni-tor effluents and the production of poisons (neutron absorbers) in the reactor core. Both these procedures depend on an accurate fission prod-uct data base. Finally the properties of the short-lived f sion products which are beta-delayed neutron emitters must be known to predict the kinetic behavior of thermal and fast reactors. Our program is directed toward the measurement of the total decay energies, γ-ray spectra, beta-delayed-neutron spectra, and the average β- and γ-energy releases from these isotopes. Isolation of individual nuclides is performed with rapid automated radiochemical separation procedures because these techniques yield isotopes of elements not available with the purely physical separa-tion systems currently being used.

We have completed detailed experiments aimed at the determina-tion of absolute intensities of γ rays associated with the antimony fission products. Of particular importance is ^{133}Sb in which we dis-covered the unexpectedly large population of the daughter ^{133}Te isomer. Of the 168 γ rays we observed in the ^{133}Sb decay only those with inten-sities of five percent or greater are listed in Table C-1.

---

[18] K. F. Ratcliff, Phys. Rev. C3, 117 (1971).

[19] S. M. Grimes, C. H. Poppe, C. Wong, and B. J. Dalton, Phys. Rev. C18, 1100 (1978).

Table C-1. Absolute intensities of γ rays above 5% absolute
            intensity for [133]Sb decay.

E_γ	I_γ
keV	per cent
817.8 (4)[a,b]	13.0 (1.1)
836.88 (7)	7.9 (1)
1096.22 (3)	100 (3)
1728.59 (7)	6.0 (4)
2416.2 (8)	6.0 (1.1)
2755 (1)	8.8 (1.4)

[a] Numbers in parenthesis are uncertainties in the last
    figure(s).

[b] Several γ rays of this energy are observed for antimony.

Table C-2. Comparison of experimental and calculated absolute
            delayed-neutron yields.

Nuclide	Observed Yield %	Calc. Yield This work %
[232]Th	5.27 ± .40	5.24
[232]U	0.44 ± .03	0.45
[233]U	0.74 ± .04	0.79
[238]U	4.60 ± .25	4.43
[237]Np	1.07 ± .10	1.04
[238]Pu	0.46 ± .07	0.43
[239]Pu	0.65 ± .05	0.68
[241]Pu	1.57 ± .15	1.57
[242]Pu	1.97 ± .233	2.46
[241]Am	0.51 ± .06	0.45
[242m]Am	0.69 ± .05	0.69
[245]Cm	0.59 ± .04	0.75
[249]Cf	0.27 ± .02	0.36

2. __Fission Products with γ Rays up to 9 MeV and Ge(Li) Detector Calibrations__ (Henry, Lin, and Meyer)

We have identified and isolated fission products with γ rays of up to 9 MeV, e.g., from the decay of 5-s [84]As. In order to determine their relative intensities we have had to recalibrate a large volume Ge(Li) detector against the thermal neutron capture γ rays of chlorine and chromium. The general shape of the efficiency curve to 10 MeV has been questioned in the literature by McCallum and Coote.[20] Our calibration curve is in general agreement with theirs.

3. __Time Dependent Beta-Delayed Neutrons from Fissioning Systems__ (Waldo, Karam,* and Meyer)

We have used a ^{3}He ionization chamber in computer-controlled rapid rabbit transit system to measure the time-dependent β-delayed neutron yields. The time-dependent gross neutron counts were analyzed in a least-squares manner to obtain a few (4-6) group analysis. Gross β-delayed neutron yields (relative to ^{235}U) were obtained for ^{232}Th, ^{232}U, ^{233}U, ^{238}U, ^{237}Np, ^{238}Pu, ^{239}Pu, ^{241}Pu, ^{242}Pu, ^{241}Am, ^{242m}Am, ^{245}Cm, and ^{249}Cf. These data were compared with results calculated using a simple Z_p model of the form

$$Z_p = 0.4153A - 1.19 + 0.167 \left(236 - 92 \frac{A_c}{Z_c} \right) \quad A < 116$$

$$Z_p = 0.4153A - 3.43 + 0.243 \left(236 - 92 \frac{A_c}{Z_c} \right) \quad A > 116$$

where A_c and Z_c are the composite mass and charge of the fissioning nuclide and A is the mass of the fission product in question. The results from our calculations and experiments are compared in Table C-2.

D. FISSION PHYSICS

1. __Fission Barriers of Rotating Nuclei__ (Mustafa, Baisden, and Chandra)

We have calculated fission barriers of beta-stable nuclei as a function of angular momentum in a modified rotating liquid-drop model

---

*Georgia Institute of Technology, Atlanta, GA.

[20] G. J. McCallum and G. E. Coote, Nucl. Instr. & Methods __124__, 309 (1975).

(MRLDM).[21] The calculation covered the mass range from 20 to 260 and the angular momentum range from zero to the limiting value, at which point the fission barrier disappears. The model used in the calculation is macroscopic (no shell effects) and it is similar to the rotating liquid drop model (RLDM) of Cohen, Plasil, and Swiatecki.[22] Unlike RLDM, our model incorporates the finite range of nuclear force and the diffuse nuclear surface, as in the Yukawa-plus exponential model of Krappe, Nix, and Sierk.[23]

The calculated fission barriers have been compared with the predictions of RLDM. In general, the fission barriers in our model are lower than those of RLDM, and we have found up to 25 per cent difference in the predictions of the two models. These predictions can be tested by heavy-ion reaction studies and utilized in a statistical-model calculation of the deexcitation of a compound nucleus by particle emission and fission.

E.   DATA EVALUATION AND COMPILATION

1. Evaluation of Neutron Interactions with ^{209}Bi (Howerton and Smith*)

Neutron interactions with ^{209}Bi have been evaluated from $E_n = 10^{-11}$ to 20 MeV in response to requests from the magnetic fusion energy community. The evaluated data, in ENDF/B format, are available from the National Nuclear Data Center.

2. Atlas of Photoneutron Cross Sections (Berman)

A supplement to the Bicentennial Edition of the Atlas of the Photoneutron Cross Sections Obtained with Monoenergetic Photons, including recent data on ^{13}C, ^{18}O, ^{55}Mn, ^{59}Co, ^{186,188,189,190,192}Os, ^{232}Th, and ^{235,236,238}U, was issued in 1979 (UCRL-78482 Supp.) A new edition, including more recent data on ^{3}H, ^{3}He, ^{4}He. and ^{17}O, and expanded to include graphs of the running sums of the integrated cross sections and their first and second moments, is in preparation and will be published in Atomic Data and Nuclear Data Tables.

---

*Argonne National Laboratory, Argonne, IL 60439.

21 P. A. Baisden, M. G. Mustafa, and H. Chandra, Bull. Am. Phys. Soc. (Series II), 24, 815 (1979).

22 S. Cohen, F. Plasil, and W. J. Swiatecki, Ann. Phys. (N.Y.) 82, 557 (1974).

23 H. J. Krappe, J. R. Nix, and A. J. Sierk, Phys. Rev. C20, 992 (1979).